Vol. 25(4):437-446 | Ocean and Polar Research | December 2003

Article

Field Measurements of Wave Directionality in Water of Finite Depth

Constantine Memos* **and Athanassios Ziros**

School of Civil Engineering, National Technical University of Athens, 15780 Zografos, Greece

Abstract : Field measurements of directional waves were carried out during the summer of 2002 at two coastal sites in water of finite depth. A couple of general purpose instruments were used employing acoustic Doppler technology. The aim of the study was to investigate the spatial behavior of the directional movement of waves as they come ashore. In total, 74 tests were carried out during which sea states of low to moderate intensity were recorded. A great number of these runs displayed bimodal characteristics of the spreading function at high frequencies. It was found that in general, the frequency-integrated directional width tends to broaden as the water shoals and when refraction effects are negligible. This is attributed to wave-wave interactions that become pronounced in shallow water. The same directional width showed, also, a tendency to increase with increasing peak frequency of the sea state spectrum. The behavior of the kurtosis of the spreading function was also examined. It was found that for higher frequencies this index tends to increase in wave spectra above a certain sea severity threshold.

Key words : wave directionality, transitional water, energy spread

1. Introduction

The energy spread among the various spectral frequencies and directions of wind waves is a characteristic of great importance for many coastal engineering problems. The associated directional spectrum represents the wave field more fully as compared to the conventional one-dimensional frequency spectrum. Most field experiments have so far focused on collecting wave directionality data in deep water. It is, however, obvious that knowledge of this information in intermediate or shallow water, where most coastal sediment transport is taking place and the majority of maritime structures are built, would be invaluable.

The present study is aimed at collecting wave directionality data in coastal waters in order to investigate the relevant characteristics of the incoming wave field. To this end, a user-friendly procedure was developed by employing low-cost field measuring equipment. The measurements were conducted at two locations in Greek coastal waters during the summer of 2002, by using a couple of submerged PUV wave-current meters manufactured by Nortek AS. The collection of data simultaneously by two identical instruments deployed at different depths enabled us to draw some preliminary results regarding the modification of the directionality characteristics as the waves approach the shore.

The material presented in this paper is arranged as follows: Section 2 contains the relevant background theory; section 3 is devoted to field measurements and their processing; in section 4, some representative results are presented and discussed; finally, the conclusions appear in section 5.

*Corresponding author. E-mail : memos@hydro.ntua.gr

2. Theoretical background

Wave directionality in deep water

The mechanical energy of wind waves is distributed among both frequencies of the power spectrum and horizontal directions. Wave directionality is commonly represented by the directional spectrum $S(f, \theta)$, a function of frequency f and angle of propagation θ. Use of this spectrum gives more realistic results, especially in coastal

waters, and, is therefore pertinent for studying coastal processes and designing relevant structures (CERC 1985). It has been estimated that the corresponding one-dimensional spectrum $S(f)$ can yield higher values of the significant wave height, as compared to the corresponding ones produced by $S(f, \theta)$, by up to 20% (Collins *et al.* 1981). It is customary to assume that the directional spectrum can be deduced from $S(f)$ by the following relation:

$$S(f, \theta) = D(f, \theta)\, S(f) \tag{1}$$

where the directional spreading function $D(f, \theta)$ must obey the normalization condition:

$$\int_{-\pi}^{\pi} D(f, \theta) d\theta = 1 \tag{2}$$

Relation (2) suggests that $D(f, \theta)$ can be regarded as a joint probability density function denoting the distribution of wave energy among the pairs $<f, \theta>$. Thus, various statistics can be defined as follows.

- Mean wave direction for any given frequency f:

$$\theta_m(f) = \int_{-\pi}^{\pi} \theta D(f, \theta) d\theta \tag{3}$$

- Principal wave direction for any given frequency f:

$$\theta_p(f) = \Theta \text{ for which } D(f, \Theta) = \max \tag{4}$$

- Directional variance for any given f or equivalently energy spread around $\theta_m(f)$:

$$\sigma_o^2(f) = \int_{-\pi}^{\pi} [\theta - \theta_m(f)]^2 D(f, \theta) d\theta \tag{5}$$

- Skewness of $D(f, \theta)$ for any given f:

$$\gamma_1(f) = \sigma_o^{-3}(f) \int_{-\pi}^{\pi} [\theta - \theta_m(f)]^3 D(f, \theta) d\theta \tag{6}$$

- Kurtosis of $D(f, \theta)$ for any given f:

$$\gamma_2(f) = \sigma_o^{-4}(f) \int_{-\pi}^{\pi} [\theta - \theta_m(f)]^4 D(f, \theta) d\theta \tag{7}$$

The difference between the values of θ_p and θ_m is normally less than 0.2 rad. Greater differences denote increased skewness of $D(f, \theta)$. Field measurements by Kumar *et al.* (2000) showed large values of $|\theta_p - \theta_m|$ in sea states rich in high frequency content.

The directional spreading function should exhibit periodicity with respect to the angular variable θ. This is safeguarded by analyzing $D(f, \theta)$ in the form of a Fourier series, as will be shown in the following section.

Despite the stochastic character of the spreading function, a number of analytical expressions for $D(f, \theta)$ have been proposed. Pierson *et al.* (1955) made the first attempt by proposing a directional spreading function independent of frequency:

$$D(f, \theta) \equiv D(\theta) = \frac{2}{\pi} \cos^2 \theta, \quad |\theta| \le \frac{\pi}{2} \tag{8}$$

where θ is the angular deviation from the principal wind direction.

Since then several investigators have proposed analytical expressions for $D(f, \theta)$ (Borgman 1969; Nagai 1972; Borgman 1984; Donelan *et al.* 1985; Banner 1990). However, the relation most frequently used is based on the field measurement analysis by Longuet-Higgins *et al.* (1963):

$$D(\theta) = N(s) \cos^{2s}\left(\frac{\theta}{2}\right) \tag{9}$$

where $N(s)$ is the normalisation factor, s parameter, and θ the angle formed with the principal direction. In order that condition (2) be satisfied, the previous relation yields:

$$N(s) = \frac{1}{\pi} 2^{2s-1} \frac{\Gamma^2(s+1)}{\Gamma(2s+1)} \tag{10}$$

where Γ is the gamma function.

The parameter s adapts the peakedness of $D(\theta)$ to the local conditions and as such it can be seen as providing in a way the missing dependence of D on the wave frequency f. This fact has been exploited further by various researchers. Mitsuyasu *et al.* (1975), proposed an explicit dependence of s on wave frequency:

$$s = 11.5 (c_p / U)^{2.5} \left(\frac{f}{f_p}\right)^b \tag{11}$$

where c_p is the phase speed at the spectral peak, U is the wind speed at a height 10 m above sea level, and $b = 5$ for $f/f_p < 1$ or $b = -2.5$ otherwise.

An alternative simpler expression for s was proposed by Goda and Suzuki (1975):

$$s = s_{\max} (f/f_p)^b \tag{12}$$

where $s_{\max} = 10$ for wind waves

$s_{\max} = 25$ for swell generated at a small distance

$s_{\max} = 75$ for swells coming from a large distance.

Hasselmann *et al.* (1980) considered pitch/roll buoy data and proposed the following values for s:

$$s = \begin{cases} 6.97(f/f_p)^{4.06}, & f < 1.05f_p \\ 9.77(f/f_p)^{\mu}, & f \geq 1.05f_p \end{cases} \quad (13)$$

where $\mu = -2.33 - 1.45\left(\frac{U}{c_p} - 1.17\right)$.

It was subsequently found (Donelan *et al.* 1985) that the wave age c_p/U does not affect the value of the parameter s decisively. Thus expression (12), given its simplicity, has found wider application than relations (11) and (13).

Finally, Wang (1992) related s to the significant wave height H_s and to the wavelength L_p at the peak frequency:

$$s = 0.2\ (H_s/L_p)^{-1.28}\ (f/f_p)^b \quad (14)$$

with b taking the same values as in eq. (11).

Wave directionality in water of finite depth

The evolution of the directional wave spectrum can in general be expressed as follows (Willebrand 1975):

$$\frac{DS(f,\theta)}{Dt} = S_{in} + S_{ne} + S_{ds} + S_b \quad (15)$$

Where S_{in} is wind input, S_{nl} nonlinear wave-wave interactions, S_{ds} dissipation due to wave breaking, and S_b bottom friction. It appears that nonlinear terms play a dominant role in shaping the directional spreading in deep water (Banner and Young 1994). The same term seems to be responsible in water of finite depth for the smoother distribution in space of the energy dispersion, resulting in a broader directional dispersion function (Young *et al.* 1996). This trend, quite evident in transitional water, can be reversed in very shallow water. The issue of whether or not the spreading function broadens as the waves move from deep to shallow water has not been fully resolved yet. Thus, the main objective of the present study was to collect data that would provide more insight into this topic.

When waves travel in water of finite depth, the three last source terms of eq. (15) depend on the site specific bed topography of the area under consideration. Therefore, any expressions of the directional dispersion function cannot have general applications in water of finite depth. Given this limitation, Young *et al.* (1996) provided a formulation for parameter s that fits data for wave propagation in transitional water of a nearly constant depth:

$$s = 11(f/f_p)^{\kappa} \quad \kappa = 2.7 \text{ for } f < f_p \quad \kappa = -2.4 \text{ otherwise} \quad (16)$$

The above expression when compared with the corresponding results by Donelan *et al.* (1985) suggests that at

(a)

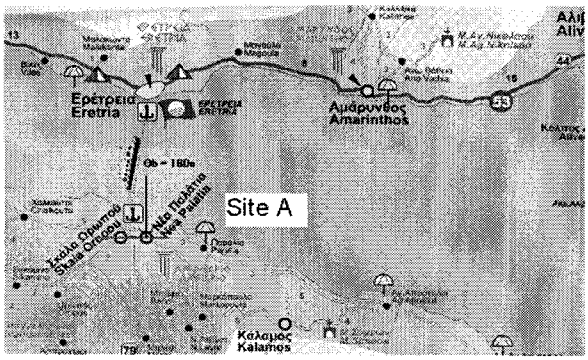

(b)

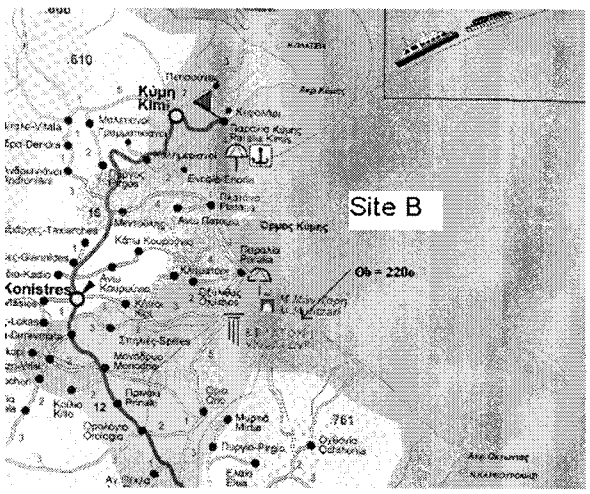

(c)

Fig. 1. Location of field measurements sites.

finite depths, the energy spreading can be broader than in deep water. Since refraction had an insignificant effect on the above data, the broadening of the directional spread in water of finite depth was attributed to nonlinear wave-wave interactions.

3. Field measurements and data processing

Sites of data collection

Field measurements were collected at two coastal sites of Central Greece. Site A was located in quite protected waters, while site B faced the open Aegean Sea (Fig. 1). Both locations were selected for displaying a more or less straight shoreline, uniform bed topography with mild slopes, and an orientation open to the north sector, which is active in winds during summer, the period of the year for which the fieldwork was planned to take place. The bed topography of the selected sites minimized to a large extent the refraction effects of waves whose incidence was normal. Site A stretched along the E-W axis with a maximum effective fetch to the NE and NW some 20 km. The seabed was sandy with a uniform slope of 5%. The shore of site B extended along a NW-SE axis for about 12 km. The fetches to the north sector were longer than 100 km, while the seabed sloped uniformly at about 15%.

Instruments used

Data collection was performed by employing two identical Aquadopp devices, i.e. bottom mounted probe, 57 cm long and 7.5 cm in diameter, capable of recording, among other parameters, the free surface geometry as it evolves in time. This is achieved through a pressure and velocity approach (PUV) improved considerably during the past decade (Gordon and Clarke 1999). The time series of the absolute pressure is recorded as well as the corresponding series of the three components of the velocity vector within a specified finite volume of the fluid close to the free surface. These velocities are determined by the Doppler effect on three sound waves emanating from the head of the probe. The data are stored in an internal memory of 2 MB and can be downloaded afterwards onto a PC. By suitably processing the above recordings, one can readily obtain the one-dimensional spectrum $S(f)$ and the directional spreading function $D(f, \theta)$. These instruments although not very accurate are quite practical and cost-effective in measuring wave characteristics. The pressure sensor displays an accuracy of 1-2 mm, the maximum angular error of the wave direction is of the order of 1-2°, and the noise level in the velocity spectrum is 3×10^{-3} m^2/sec. (Gordon and Lohrmann 2001). The minimum water depth where the probe can be operable is 2 m. The lower cut-off period of the measured waves is close to 2 sec.

Data acquisition

Measurements of pressure and velocity were taken simultaneously by two of the above-mentioned devices deployed in transitional waters along the same as far as possible, ray of the prevailing wave system. The time distance between the two probes was about 2-3 sec in terms of the phase speed of the significant wave. Events with the minimum possible refraction effects were picked for data collection, since wave refraction tends to modify the orientation of the wave components directly, hence the directional spread function too.

The field campaigns took place during the period 15 July 2002 to 25 August 2002. The time series of the measured variables by both probes in a single run had a length of 1025 sec and the sampling rate was 1 Hz. The resulting database contained 41 runs as shown in Table 1.

Table 1. Log-book of tests.

Site	Date	Start time	Finish time	Number of runs
A	17/7/02	19:10	19:50	2
	27/7/02	19:30	20:30	3
	3/8/02	19:50	20:50	3
B	10/8/02	11:45	13:05	4
A	13/8/02	19:35	20:35	3
	14/8/02	20:07	20:47	2
B	17/8/02	13:52	16:32	8
A	19/8/02	19:00	20:00	3
B	24/8/02	11:55	14:15	8*
		16:30	18:10	5

*single probe

Data processing

The one-dimensional spectrum is calculated through the pressure recording for waves with periods T > 7 sec, while in the case of smaller waves, the time series of the orbital velocities is used. The pressure spectrum at depth h is translated into the conventional power spectrum of the free surface through its multiplication by the factor $\left[\frac{\cosh kh}{\cosh k(h+y)}\right]^2 \cdot \frac{1}{\rho_w^2 g^2}$. The corresponding factor for the horizontal velocity spectrum is $\left[\frac{\sinh kh}{\cosh k(y+h)}\right]^2 \frac{1}{f^2}$ (Gordon and Clarke 1999).

In cases where there is a current of appreciable velocity present, then the following correction to the dispersion relation takes place through the relevant software:

$$\omega = (gk\tanh kh)^{1/2} + kU\cos a \tag{17}$$

where U is the mean current velocity, α is the angle between the current and the propagation of waves. The above correction is effected automatically when the second term of relation (17) becomes comparable with the first; this is assumed to hold when the following inequality is satisfied, i.e.

$$U\cos a \geq 0.14\left(\frac{g}{k}\tanh kh\right)^{1/2} \tag{18}$$

The minimum wave height that can be recorded with acceptable accuracy, as described by the Nyquist frequency, depends on both the wave period and water depth. Thus, for a depth of $h = 5$ m and a wave period of $T = 3.6$ sec, the minimum significant wave height is $H_s = 0.10$ m; for $h = 10$ m and $T = 5$ sec, the corresponding figure is $H_s = 0.20$ m. The various parameters of the wave field are deduced from the moments m_i of the power spectrum through the standard expressions, e.g. mean angular frequency $\omega = m_1/m_0$, significant wave height $H_s = 4\ m_0^{1/2}$, etc.

The directional spectrum is obtained from the one-dimensional one through its multiplication by the corresponding directional spreading function $D(f, \theta)$. This can be determined by a number of methods, e.g. the parametric spectral method or PSM (Longuet-Higgings *et al.* 1963), the maximum likelihood method (Capon 1969), the maximum (or extended maximum) entropy method (Nwogu 1989), etc. The data processing software used (WavePro) is based on the PSM. According to this method, $D(f, \theta)$ is analysed into a Fourier series, safeguarding thus its periodicity with respect to θ:

$$D(f,\theta) = \frac{1}{2\pi}\left[1 + 2\sum_{n=1}^{\infty} a_n(f)\cos n\theta + b_n(f)\sin n\theta\right] \tag{19}$$

where the Fourier coefficients are expressed through:

$$a_n = \int_o^{2\pi} D(f,\theta)\cos n\theta d\theta, \quad b_n = \int_o^{2\pi} D(f,\theta)\sin n\theta d\theta$$

Values of these coefficients can be obtained by the auto-spectra or the co-spectra of the available time series. By using the pressure (p) and the orbital velocity data (analysed into u- and v-components), the first four coefficients can be derived as follows (Kuik *et al.* 1988):

$$a_1(f) = \frac{C_{pu}(f)}{kC_{pp}(f)} \tag{20}$$

$$b_1(f) = \frac{C_{pv}(f)}{kC_{pp}(f)} \tag{21}$$

$$a_2(f) = \frac{C_{uu}(f) - C_{vv}(f)}{k^2 C_{pp}(f)} \tag{22}$$

$$b_2(f) = \frac{2C_{uv}(f)}{k^2 C_{pp}(f)} \tag{23}$$

where C_{ii} denotes the auto-spectrum, C_{ij} co-spectrum and $k = \left(\frac{C_{uu} + C_{vv}}{C_{pp}}\right)^{1/2}$. Given the four first Fourier coefficients, the statistics of $D(f, \theta)$ can be deduced by the following expressions (Mardia 1972):

$$\theta_m(f) = \arctan(b_1/a_1) \tag{24}$$

$$\theta_p(f) = \frac{1}{2}\arctan(b_2/a_2) \tag{25}$$

$$\sigma_o = [2(1 - m_1)]^{1/2} \tag{26}$$

$$\gamma_1 = -n_2\left[\frac{1}{2}(1 - m_2)\right]^{-3/2} \tag{27}$$

$$\gamma_2 = (6 - 8m_1 + 2m_2)\sigma_o^{-4} \tag{28}$$

where parameters m_1, m_2, n_2 are deduced from the Fourier coefficients as follows:

$$m_1 = (\sqrt{a_1} + \sqrt{b_1})^{1/2}$$
$$m_2 = a_2\cos 2\theta_m + b_2\sin 2\theta_m$$
$$n_2 = b_2\cos 2\theta_m - a_2\sin 2\theta_m$$

It is noted that expression (26) is deduced from the non-periodic relation (5) by substituting $(\theta - \theta_m)^2$ by $2\ [1 - \cos(\theta - \theta_m)]$, a good approximation when $\theta - \theta_m$ is small. The above expressions hold for any given frequency f. To obtain a representative value within a range of frequencies $[f_1, f_2]$, a weighted average is calculated, having weights the values of $S(f_i)$ (Van der Vlugt *et al.* 1981). Thus, for θ_m the following relation holds:

$$\theta_m[f_1, f_2] = \int_{f_1}^{f_2} \theta_m(f)S(f)df \Big/ \int_{f_1}^{f_2} S(f)df \tag{29}$$

At the limits $f_1 \to 0, f_2 \to \infty$, the mean direction refers to the whole wave field. Similar expressions hold for the rest of the statistical quantities. The above relation enables the discretization of the frequencies into bands, e.g. the

ones used in the present study: 0.1-0.2 Hz, 0.2-0.3 Hz, 0.3-0.4 Hz, 0.4-0.5 Hz. Thus, results can be obtained for each particular frequency band in addition to results for the whole range, e.g. 0.1-0.5 Hz. The steps used for the discretization of the equations was 0.01 Hz for the frequencies and 0.17 rad for the angles. The collected data represented transitional water depth as defined by linear wave theory, i.e. $1/4 < kh < \pi$. This is shown in Fig. 2, where the distribution of $k_p h$ values is given for the data set, with k_p denoting the wave number at the spectral peak and h the water depth.

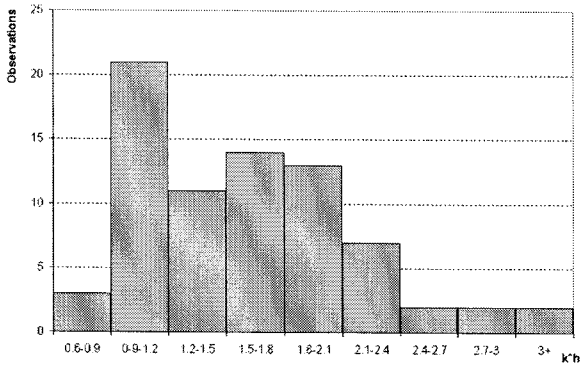

Fig. 2. Distribution of $k_p h$ of the collected data over the number of tests performed.

4. Results and discussion

For each field test, the following results were provided:

- The one-dimensional spectrum $S(f)$ and its parameters.
- Representation of the directional spread function $D(f, \theta)$ along with its angular characteristic, its variance, and cross-sections $D(f_i, \theta)$ along with the characteristic values f_i coinciding with the local extremes of $S(f)$.
- Diagrams of θ_m, σ_o, γ_1, γ_2, referred to $D(f, \theta)$ and its predetermined frequency bands.
- Contour plots of the two-dimensional spectrum $S(f, \theta)$.

Analysis of the above results revealed some interesting points mainly in the behavior of the directional spreading function $D(f, \theta)$. It was found that there is a tendency of the variance of $D(f, \theta)$ to increase with decreasing depth, meaning that finite depth wind wave spectra tend to be "broader" than the corresponding deep water ones. Fig. 3 depicts data from all runs that show this weak but clear connection between σ_{om} and h. The term "broader" should be conceived in this context with regard to the spread of the wave energy more evenly in more directions, implying a lower directional exponent s. This does not necessarily

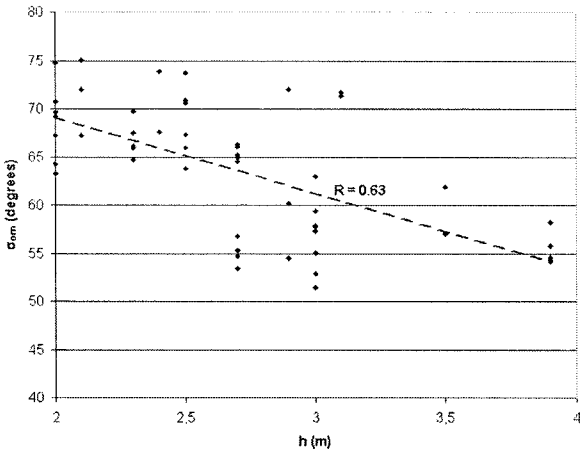

Fig. 3. Variation of σ_{om} at different depths.

lead to broader spectra in the strict mathematical sense. Variable σ_{om} denotes a weighted (with to respect to $S(f_i)$) average value of σ_o (f_i) for the specified frequency bands mentioned above.

The above-mentioned tendency is difficult to detect due to the relative proximity of the two measuring points; also due to the presence of refraction effects that act in the opposite sense, tending to narrow the directional spreading. These effects could not be totally removed although attempts were made to minimize them. This may explain to a certain extent the considerable scatter of the graph points in Fig. 3. The broadening of the directional spread is attributed to nonlinear wave-wave interactions, which increase their strength as the water depth decreases. It is well established that despite the fact that as the waves move into shallower water, the effect of quadruplet interactions diminishes considerably, the overall nonlinear wave-wave interactions increase their contribution to the energy balance in such waters, due to the enhanced triad resonance effects. It is noteworthy that Young *et al.* (1996) have come to similar conclusion, i.e. directional broadening occurs because, as the water depth decreases, wave number components, separated by progressively larger angles, can satisfy the resonance conditions and potentially interact with them nonlinearly. They also showed that one-dimensional spectra decay more gradually according to frequency changes as the water depth decreases. This leads in general to higher σ_o as will be shown in the following. Herbers *et al.* (1999) also demonstrated an increase in the directional spread of waves in shallow water whenever wave breaking occurs intensively.

The mean directional variance σ_{om} presents an improved correlation, over the one shown in Fig. 3, with a peak

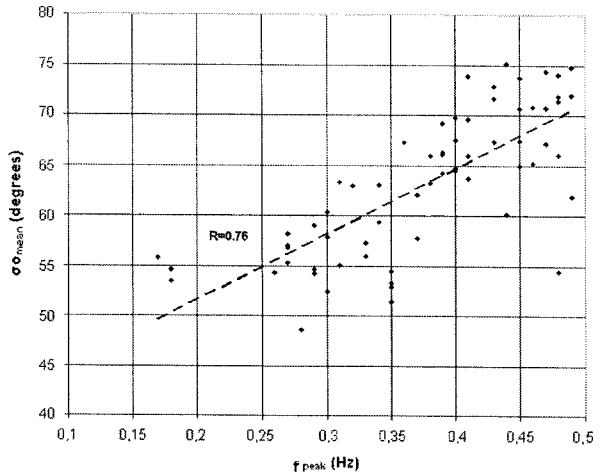

Fig. 4. Relation of $\sigma_{\theta m}$ with f_p.

frequency f_p irrespective of water depth. This is shown in Fig. 4 where 65 tests are included.

The above results refer to the compound directional width $\sigma_{\theta m}$ as defined earlier and cannot be directly compared with existing results by various investigators that examine the behavior of the directional width σ_θ (f) with respect to frequency within the same sea state. However, the general trend of increased directional width with frequency is in line with other studies, e.g. with results by Kuik and Holthuijsen (1981), or by Kumar *et al.* (2000). This trend is, nevertheless, valid for frequencies higher than f_p, but in most cases this frequency band ($f/f_p > 1$) contains the greater part of wind wave energy in coastal waters.

The broadening of the directional dispersion of waves in transitional waters under conditions of negligible refraction is also illustrated by the modification of $D(f, \theta)$ as the waves propagate inshore. Fig. 5 presents a graph of $D(f_p, \theta)$ for two different depths produced from a test (24-8-2003, 16:30) undertaken at site B.

The one-dimensional spectra corresponding to the same sea conditions and depth with Fig. 5, are presented in Fig. 6. It appears from these graphs that the spectrum widens slightly in the shallower position. In fact, the calculated values of the spectral width parameter ν, show an increase of 12% from deeper water ($h = 3.9$ m) to the shallower ($h = 2.7$ m) location. It is remembered that the value of ν is expressed by (Longuet-Higgings 1957):

$$\nu^2 = \frac{m_o m_2}{m_1^2} - 1 \tag{30}$$

In most tests, the increase of directional variance due to

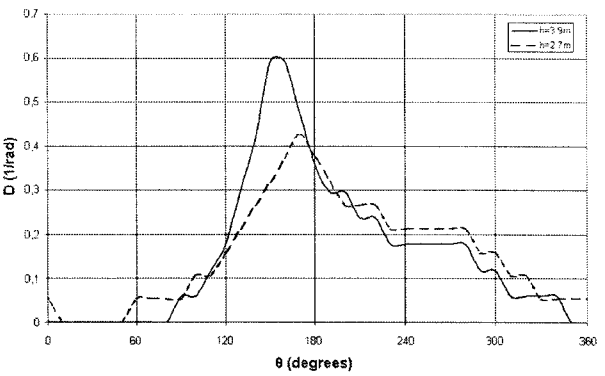

Fig. 5. Modification of D (f_p, θ) due to depth variation.

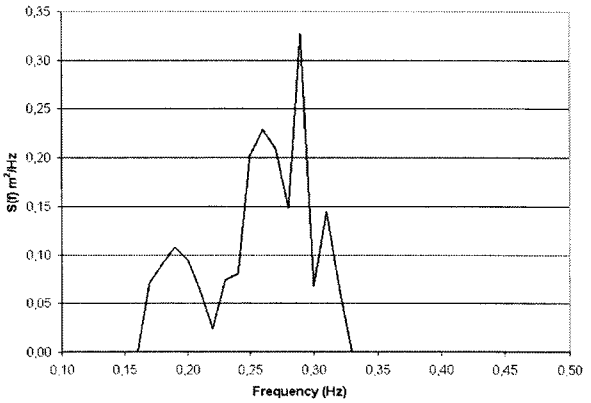

(a)

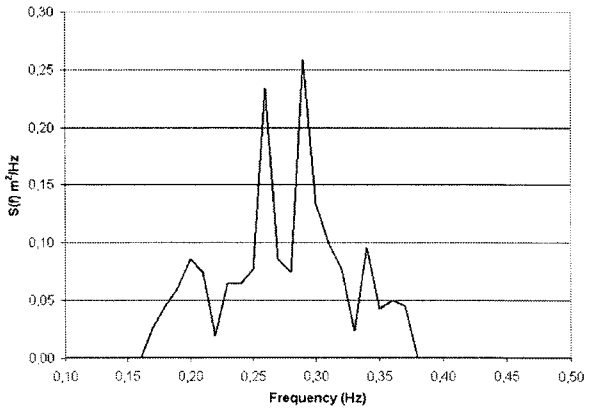

(b)

Fig. 6. Wave spectra at depths: h=3.9 m (a); h=2.7 m (b).

shoaling water was accompanied by a widening of the one-dimensional spectrum, expressed by a corresponding increase of parameter ν. Although the signified relation between σ_θ and ν is weak, the general trend is that, under the conditions stated, the spectral width increases as the water shoals. This can be largely attributed, as in the case

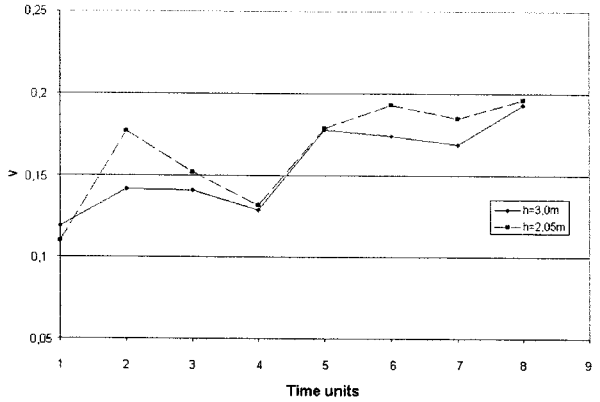

Fig. 7. Values of ν at two water depths.

of directional variance, to nonlinear wave-wave interactions that are more pronounced in shallow rather than in deep water. Fig. 7 shows such a trend in terms of the parameter ν representing 8 rather narrow band sea states in site B.

The behavior of the angular distribution function was found to depend on the actual values of peak frequency. For 14 runs out of a total of 17 runs in site B with a mean frequency $f_m < 0.3$ Hz roughly, it was found that the bulk frequency-integrated kurtosis in band $f/f_p > 1$ was greater than the corresponding value for $f/f_p < 1$. The inequality between the two values of kurtosis was found to be stronger for sea states of higher f_p. Milder sea states recorded at both sites displayed the reverse trend in 79% of the runs. The above finding agrees with results by Kuik and Holthuijsen (1981) for the frequency related kurtosis $\gamma_2(f)$ in combination with the relevant frequency spectrum. It is noted that their results refer mainly to a unimodal spread function in contrast with the present study, where a lot of data comes from bimodal directional distributions.

No similar trend was detected for the skewness γ_1.

A lot of the field measurements displayed a directional bimodality in the spread function. This can be verified by the bulk values γ_1, γ_2, of the recorded runs as compared to the criteria defining the domain where the unimodal and symmetric spreading should lie (Kuik *et al.* 1988). According to these, the unimodal domain is defined by the following inequalities:

$$\begin{array}{ll} \gamma_2 > 2 + |\gamma_1|, & |\gamma_1| < 4 \\ \gamma_2 > 6 & \text{otherwise} \end{array} \qquad (31)$$

The majority of the recorded runs provided data that fell outside the unimodal domain or around the borderline defined by the above criteria. The second direction may be due to the reflection of some of the swell energy from the coast. The existence of the bimodal distribution function at certain frequencies is also illustrated in the comparison between the directions θ_p and θ_m. It is known (Kumar *et al.* 2000) that in general, the values of θ_p and θ_m are almost identical in unimodal directional distributions. Fig. 8 shows the relationship between mean and principal directions for sites A and B, suggesting to a certain extent the directional bimodality of some of the recorded sea states.

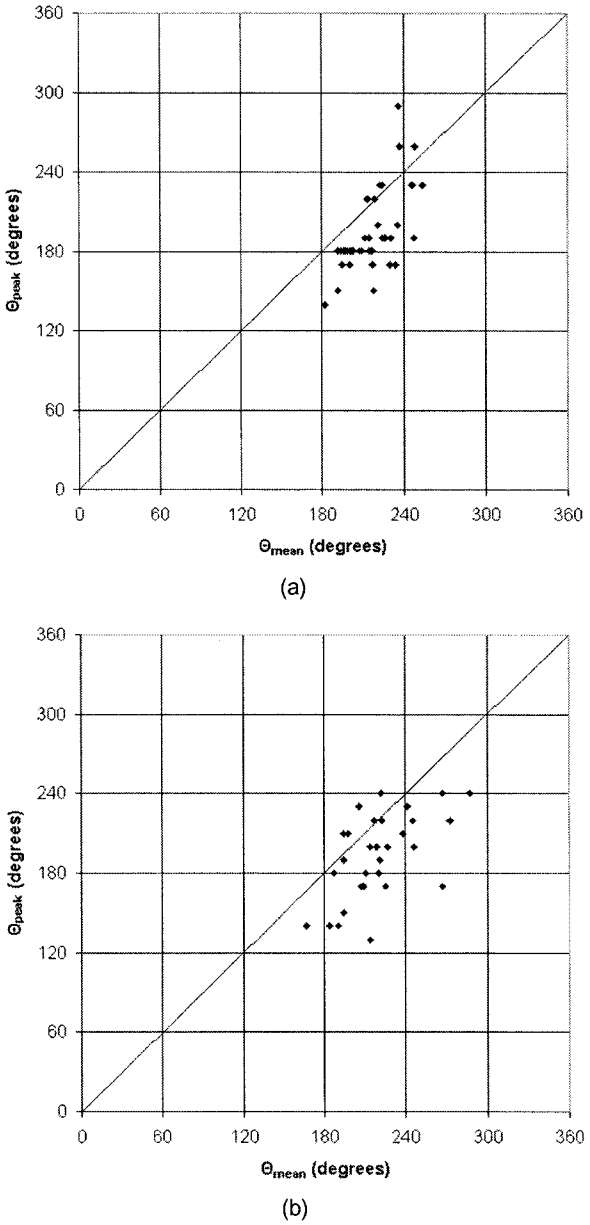

Fig. 8. Relationship between θ_p and θ_m : (a) Site A ; (b) Site B.

5. Conclusions

A set of field measurements comprising 74 tests was carried out during the summer of 2002 at two sites in Greek coastal waters of intermediate depth. Two identical bed-mounted instruments were used employing the Doppler effect on generated sound waves. The pressure and velocity approach was used to obtain, through mathematical processing of the data, the directional spreading function and the directional wave spectra. The recorded sea states were of low to moderate energy, many of them displaying a bimodal directional spread. For this reason the statistics of the spreading function were investigated and not the actual function itself. It was found that:

(i) Frequency-integrated directional width tends to increase in shoaling water whenever the refraction effects are negligible. This is attributed mainly to nonlinear wave-wave interactions that become more pronounced as the water depth decreases. This is a justifiable assertion, since, as the water shoals, the high frequency content of the wave spectrum is enriched due to wave-wave interactions. It is also known that high frequencies are associated with broader directional width, thus leading to higher frequency-integrated directional width. Under the same conditions of minimal refraction, it was found that the wave spectrum broadens in general as the waves come ashore. This is attributed to the same mechanism described above. However, the issue of spectral width was not fully investigated.

(ii) The above directional width tends to increase with increasing peak frequency of the spectrum.

(iii) The kurtosis of the spreading function associated with frequencies $f > f_p$ in a given sea state is higher than the corresponding value for $f < f_p$. This is generally true for sea states with values of $f_m < 0.3$.

Past investigations have arrived at result (i) above for unimodal spread function. The present study, covering bimodal cases as well, suggests that this finding can be of more general validity.

References

Banner, M.L. 1990. Equilibrium spectra of wind waves *J. Phys. Oceanogr.*, 20, 966-984.

Banner, M.L. and I.R. Young. 1994. Modelling spectral dissipation in the evolution of wind waves-Part 1. Assessment of existing model performance. *J. Phys. Oceanogr.*, 24, 1550-1671.

Borgman, L.E. 1969. Directional spectra models for design use. *Proc. Offshore Tech. Conf.*, 1069, 721-746.

Borgman, L.E. 1984. Directional spectrum estimation for the Sxy gauges. p. 1-104. In: *Tech. Rept. CERC*, USAE Waterways Exper. Station, Vicksburg.

Capon, J. 1969. High-resolution frequency-wavenumber spectrum analysis. *Proc. IEEE*, 57, 203-219.

Coastal Engineering Research Center. 1985. Directional Wave Spectra using cosine-squared and cosine 2s Spreading Functions. *Coast. Eng. Tech.*, Note-I-28, 6/85, 6 p.

Collins, J.I., W-L. Chiang, and F. Wu. 1981. Refraction of directional spectra. p. 251-268. In: *Proc. Conf. Directional Wave Spectra Applications*. ASCE, Berkeley, CA.

Donelan, M.A., J. Hamilton, and W.H. Hui. 1985. Directional spectra of wind-generated waves. *Phil. Trans. Roy. Soc. London*, A 315, 509-562.

Gordon, L. and L. Clarke. 1999. Doppler Current Meter Wave Observations in the Near-Shore and Surf Zone. <www.inquiry.nortek.no>.

Gordon, L. and A. Lohrmann. 2001. Near shore Doppler current meter wave spectra. Proc. Waves'01, ASCE.

Hasselmann, D.E., M. Dunckel, and J.A. Ewing. 1980. Directional wave spectra observed during JONSWAP. *J. Phys. Oceanogr.*, 13, 191-207.

Herbers, T.H.C., S. Elgar, and R.T. Guza. 1999. Directional spreading of waves in the nearshore. *J. Geophys. Res.*, 104 (C4), 7683-7693.

Kuik, A.J., G. Vledder, and L.H. Holthuijsen. 1988. A method for the routine analysis of pitch and roll buoy wave data. *J. Phys. Oceanogr.*, 18, 1020-1034.

Kumar, V.S., M.C. Deo, N.M. Anand, and K.A. Kumar. 2000. Directional spread parameter at intermediate water depth. *Ocean Eng.*, 27, 889-905.

Longuet-Higgins, M.S. 1957. The Statistical Analysis of a Random, Moving Surface. *Phil. Trans. Roy. Soc. London*, A 966, 321-387.

Longuet-Higgins, M.S., D.E. Cartwright, and N.D. Smith. 1963. Observations of the directional spectrum of sea waves using the motions of a floating buoy. Ocean Wave Spectra, Prentice-Hall, N.J. p. 111-136.

Mardia, K.V. 1972. Statistics of directional data. Academic Press, London & New York.

Mitsuyasu, H., F. Tasai, T. Suhara, S. Mizuno, M. Onkusu, T. Hond, and K. Rukiiski. 1975. Observations of the directional spectrum of ocean waves using a cloverleaf buoy. *J. Phys. Oceanogr.*, 5, 751-761.

Nagai, K. 1972. Diffraction of the irregular sea due to breakwater. *Coastal Eng. Japan,* 15, 59-67.

Nwogu, O. 1989. Maximum entropy estimation of directional wave spectra from an array of wave probes. *Applied Ocean Res.*, 11, 176-182.

Pierson, W.J., Jr., G. Neuman, and R.W. James. 1955. Practical methods for observing and forecasting ocean waves by means of wave spectra and statistics. Publ. no. 603, US Naval Hydr. Office.

Van der Vlugt, A.J.M., A.J. Kuik, and L.H. Holthuijsen. 1981. The wave directional buoy under development.

p. 50-60. In: *Proc. Conf. Directional Wave Spectra Application Berkeley*, CA, ASCE.

Wang, D.W. 1992. Estimation of wave directional spreading in severe seas. *Proc. 2nd Int. Offshore & Polar Eng. Conf.*, III, 146-153.

Willebrand, J. 1975. Energy transport in a nonlinear and in homogeneous random wave field. *J. Fluid Mech.*, 70, 113-126.

Young, I.R., L.A. Verhagen, and S.K. Khatri. 1996. The growth of fetch limited waves in water of finite depth. Part 3. Directional spectra. *Coastal Eng.*, 29, 101-121.

Received Jun. 30, 2003
Accepted Nov. 10, 2003